

## Quantum Limit of Ferroelectric Phase Transitions in $\text{KTa}_{1-x}\text{Nb}_x\text{O}_3$

U. T. Höchli and H. E. Weibel

*IBM Zurich Research Laboratory, 8803 Rüschlikon, Switzerland*

and

L. A. Boatner<sup>(a)</sup>

*Ecole Polytechnique Fédérale de Lausanne, Laboratoire de Physique Expérimentale, 1007 Lausanne, Switzerland*

(Received 16 September 1977)

Dielectric and elastic constants of  $\text{KTa}_{1-x}\text{Nb}_x\text{O}_3$  are presented as a function of  $x$  and of the temperature. For  $x = 8 \times 10^{-3}$ , the system exhibits the characteristics of a ferroelectric at the displacive limit (i.e., a "quantum ferroelectric") as evidenced by three critical indices and the temperature independence of all responses near  $T = 0$ .

The investigation of structural phase transitions represents an area of inquiry which has attracted considerable attention during the past few years. Essentially, all of the previous experimental results pertinent to displacive phase transitions are characterized by the absence of discernible quantum-mechanical effects, and, therefore, the concomitant theoretical developments have proceeded, until recently, on the basis of classical mechanics. Recent theoretical work,<sup>1,2</sup> however, has indicated that at or near the so-called "displacive limit," quantum-mechanical effects can become extremely important. This "displacive limit" is defined by the set of coupling parameters for which the critical temperature  $T_c$  of the phase transition becomes equal to zero. In the classical approach, a ferroelectric is characterized by two regimes: one of dominant fluctuations (paraelectric behavior) and one of dominant dipole ordering. While the dipole-dipole interaction is usually considered to be temperature independent, the balance with short-range anharmonic interactions leads to fluctuations which decrease with decreasing temperature and ultimately allow the dipole-dipole interaction to order the crystal ferroelectrically at some temperature  $T_c$ . If  $T_c$  is in the region of zero-point lattice motion, however, decreasing the temperature does not appreciably decrease the fluctuations. As a consequence, the disordered phase may extend below its classical limit and the quantum-mechanical critical temperature is lower than the classical  $T_c$  because of the effects of zero-point motion. In the quantum limit, the temperature is an entirely ineffective parameter and the system only responds to a change in either the dipole-dipole interaction or the higher-order restoring forces. Additionally, critical exponents calculated on the basis of a quantum-mechanical model of a three-

dimensional lattice<sup>3</sup> are not equivalent to those obtained using the classical approach. In fact, the effective dimension of the lattice is increased by unity and the predictions of the quantum-mechanical "vector model" at or near the displacive limit are the same as those of mean-field theory in four dimensions. The spontaneous polarization at 0 K varies according to the equation

$$P_s(x, 0) \propto (x - x_c)^{\beta_x} \text{ with } \beta_x = \frac{1}{2}. \quad (1)$$

The inverse dielectric constant at 0 K varies as

$$\epsilon^{-1}(x, 0) \propto (x - x_c)^{\gamma_x} \text{ with } \gamma_x = 1, \quad (2)$$

and the critical transition temperature should obey the formula

$$T_c(x) \propto (x - x_c)^{1/\phi}, \quad (3)$$

where  $\phi = 2$ ;  $x$  is a general, and  $x_c$  the limiting interaction parameter.<sup>3</sup>

The purpose of this Letter is to present experimental dielectric and acoustic data which elucidate the role of quantum-mechanical fluctuations in determining the characteristics of low-temperature ferroelectric phase transitions. Critical exponents near the displacive limit are determined by fitting these data, and the results are compared with the corresponding quantum-mechanical exponents derived previously and indicated in Eqs. (1)–(3).

In the prior theoretical work dealing with quantum-mechanical effects at the displacive limit of structural phase transitions, it has been suggested<sup>1</sup> that such effects could be investigated most profitably either by employing isotropic applied pressure or by the addition of impurities to vary the sample characteristics at or near the limit. Our experiments have incorporated the latter approach, and the material  $\text{KTa}_{1-x}\text{Nb}_x\text{O}_3$  (potassium tantalate-niobate or KTN) was selected since it is

the only known example<sup>4</sup> of a cubic solid solution which undergoes a second-order transition to a ferroelectric phase whose transition temperature can be continuously varied by chemical composition over a wide range. Pure  $\text{KTaO}_3$  (i.e.,  $x=0$ ) does not undergo a ferroelectric phase transition,<sup>5</sup> but it does exhibit a dielectric anomaly near  $T=0$ . The solid solution  $\text{KTa}_{0.95}\text{Nb}_{0.05}\text{O}_3$ , however, becomes ferroelectric at about 60 K, and starting from this composition, the critical temperature increases almost linearly with increasing Nb concentration until a  $T_c$  of 700 K is obtained for pure  $\text{KNbO}_3$ .

In the system  $\text{KTa}_{1-x}\text{Nb}_x\text{O}_3$ , the Nb concentration  $x$  may be treated as an interaction parameter on the basis of the following considerations: First, in the classical limit (i.e., for  $x > 0.008$ ), the transition temperature is found to be a linear function<sup>4</sup> of  $x$ . It appears that the Nb concentration enhances the dipolar interaction since it is unlikely to influence the fluctuations of the polarization. Second, in the quantum limit, the effects

associated with increasing  $x$  resemble those resulting from external pressure. Ferroelectricity in  $\text{KTaO}_3$  has been induced<sup>6</sup> by a pressure of  $6 \times 10^8 \text{ N/m}^2$ . It has also been recognized as being mainly due to anisotropic oxygen polarizability.<sup>7</sup> It is thus reasonable to neglect the randomness of the dipolar interaction with respect to the average enhancement.

In the present work, the spontaneous polarization  $P_s$  has been measured at various temperatures from a hysteresis loop at 0.25 Hz for samples with varying Nb concentration. The low frequency of 0.025 Hz was necessary in order to ensure complete ferroelectric switching. The curves of  $P_s$  versus  $T$  have been extrapolated to 0 K, and the resulting values were used to determine the critical index  $\beta_x$ . The curves of  $\epsilon^{-1}$  versus  $T$  in Fig. 1 show that there is a minimum of  $\epsilon^{-1}$  for each sample with  $x > 0.008$ , and that the temperature at which this minimum occurs (i.e., the Curie temperature) increases with increasing  $x$ . The peculiar shape of the  $\epsilon^{-1}$  versus  $T$  curve close to  $x_c$ , however, prevents a reliable determination of  $T_c$ . An accurate determination of  $T_c$  may be made, however, by measuring the elastic compliance  $s_{11}$  using the ultrasonic resonance technique.<sup>8</sup> The same samples were employed in determining  $\epsilon^{-1}$  as a function of temperature and the results are shown in Fig. 1. The values of  $\epsilon^{-1}$  extrapolated to 0 K are shown in Fig. 2.

The elastic constant  $s_{11}^{-1}$  is plotted versus temperature in Fig. 1, and it is seen to change drastically in the same temperature range in which the dielectric maximum occurs. This change of the elastic constant is attributed to symmetry breaking of the paraelectric phase. In an ideal homogeneous sample, coupling of the strain to the order parameter leads to a step discontinuity<sup>9</sup> of the elastic constants at  $T_c$ . In an actual sample

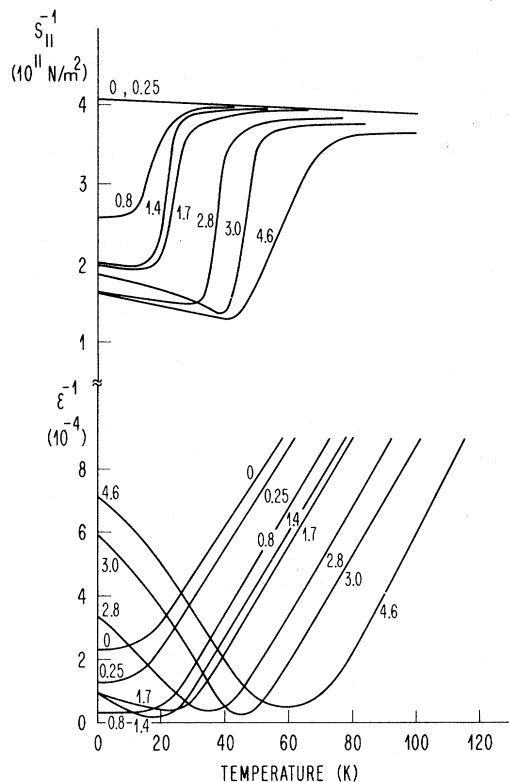


FIG. 1. The inverse of the dielectric constant and the inverse elastic compliance are shown as functions of temperature. The curves are labeled according to the Nb percentage as determined by electron microprobe analysis. Each curve contains about 50 data points.

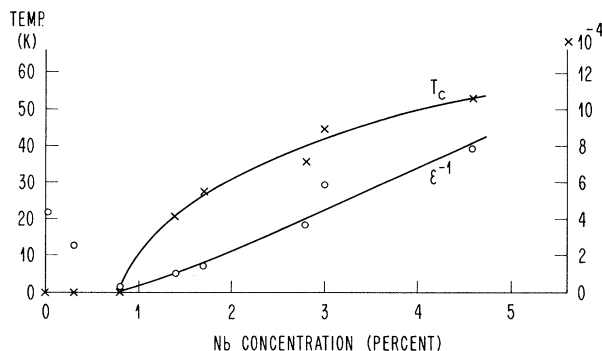


FIG. 2. Best fits of the transition line and the zero-point susceptibility by power laws.

with a long thin geometry, however, the Nb concentration is not perfectly homogeneous and  $T_c$  is changed locally. If it is assumed that the strain complies locally with constant stress, one finds an additional elastic compliance in those regions where  $T_c > T$ . If  $p(T_c)$  is the probability for a particular  $T_c$ , then

$$s_{11}(T) = s_c + \int_T^\infty dT_c p(T_c)(s_a - s_c), \quad (4)$$

when  $s_c$  and  $s_a$  are the compliances in the cubic and axial phases, respectively. From an electron microprobe analysis, it is seen that the actual Nb concentration in the KTN samples used here can be reasonably approximated by

$$p(x) = \sqrt{\pi/a} \exp[-a(x - \bar{x})^2], \quad (5)$$

The same distribution should hold for the local  $T_c$  if  $T_c$  is a linear function of  $x$  within the range of the distribution. Inserting this distribution, Eq. (5), into Eq. (4) yields

$$s_{11}(T) = \frac{1}{2}(s_a + s_c) + \frac{1}{2}(s_a - s_c) \operatorname{erf}[(T_c - \bar{T}_c)/\Delta T_c], \quad (6)$$

where

$$\operatorname{erf}(x) = \pi^{1/2} \int_0^x \exp(-t^2) dt.$$

The elastic compliances have been fitted by an error function (Fig. 3) from which the relevant parameters  $T_c$  and  $\Delta T$  are deduced.

From the width of the elastic step in the temperature scale, the sample inhomogeneity can be estimated as  $\Delta \bar{x} = (\partial x / \partial T_c) \Delta \bar{T}_c$ . The compositional inhomogeneities are generally  $\Delta \bar{x} \sim 0.003$  and are consistent with those obtained from the microprobe analysis.

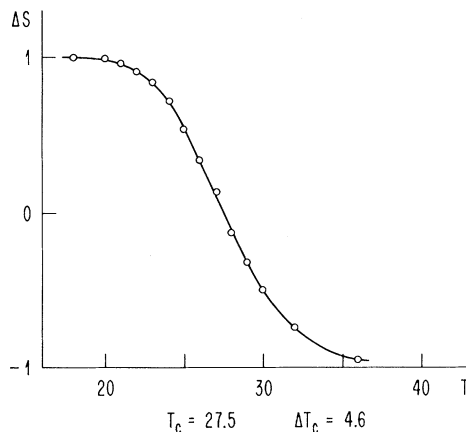


FIG. 3. Fit of elastic compliance by an error function  $\Delta S = (2s - s_a - s_c)/(s_a - s_c)$ .

One sample with  $x = 0.008$  exhibited an elastic step about one-half the size of all the others. From this, we estimated that  $x$  is distributed evenly about  $x_c$ , and thus,  $T_c(0.008) \approx 0$ . For this particular sample with  $\bar{x} \approx x_c$ , it was assumed that  $T_c \sim (x - x_c)$ , with a distribution

$$p(T_c) = \frac{1}{2} b^2 T_c \exp(-bT_c) \quad (7)$$

and with  $\int_0^\infty p(T_c) = \frac{1}{2}$ . The inhomogeneity of this sample obtained from fitting the elastic response to Eqs. (4) and (7) is also  $\Delta \bar{x} = 0.003$ . When the experimentally determined values of  $P_s(x)$ ,  $\epsilon^{-1}(x)$ , and  $T_c(x)$  are fitted to the power laws of Eqs. (1)–(3), the critical indices become

$$\phi = 1.9 \pm 0.3, \quad \gamma_x = 1.1 \pm 0.2, \quad \beta_x = 0.6 \pm 0.25,$$

and the critical Nb concentration is  $x_c = 0.008 \pm 0.0015$ . A best fit of the transition line and the zero-temperature susceptibility to corresponding power laws is shown in Fig. 2. The values for the indices  $\phi$ ,  $\gamma_x$ , and  $\beta_x$  are equal, within the experimental error, to the corresponding indices predicted by the lattice model at the quantum limit, i.e., to  $\phi = 2$ ,  $\gamma_x = 1$ , and  $\beta_x = \frac{1}{2}$ . This agreement is evidence for the validity of the vector model and the results are therefore consistent with the idea that fluctuations in the polarization do not vanish at  $T = 0$  due to the zero-point motion.<sup>5,10</sup>

For  $x$  near its critical value<sup>11</sup>  $x_c$ , both the dielectric and the elastic constants are temperature independent up to about 15 K; this indicates the temperature range of effective zero-point motion.

The authors wish to express their gratitude to Dr. J. Sommerauer for performing the measurements of the Nb concentration by electron microprobe techniques, to Mr. R. Meili for measuring the mass density, and to Dr. T. Schneider and Dr. K. A. Müller for illuminating discussions.

<sup>(a)</sup>Current address: Solid State Physics Division, Oak Ridge National Laboratory, Oak Ridge, Tenn. 37830.

<sup>1</sup>T. Schneider, H. Beck, and E. Stoll, Phys. Rev. B **13**, 1123 (1976).

<sup>2</sup>R. Oppermann and H. Thomas, Z. Phys. **B22**, 387 (1975).

<sup>3</sup>R. Morf, T. Schneider, and E. Stoll, Phys. Rev. B **16**, 462 (1977).

<sup>4</sup>C. H. Perry, R. R. Hayes, and N. E. Tornberg, *Molecular Spectroscopy of Dense Phases* (Elsevier, Amsterdam, 1976), p. 267.

<sup>5</sup>H. Burkhard and K. A. Müller, *Helv. Phys. Acta* **49**, 725 (1976), and K. A. Müller and H. Burkhard (to be published) introduce the term "intrinsic quantum paraelectric" for the analogous phenomenon observed in SrTiO<sub>3</sub>.

<sup>6</sup>H. Uwe and T. Sakudo, *J. Phys. Soc. Jpn.* **38**, 183 (1975), and earlier work quoted therein.

<sup>7</sup>R. Migoni, H. Bilz, and D. Bäuerle, *Phys. Rev. Lett.* **37**, 1155 (1976).

<sup>8</sup>G. Rupprecht and H. Winter, *Phys. Rev.* **155**, 1019 (1967).

<sup>9</sup>J. C. Slonczewski and H. Thomas, *Phys. Rev.* **131**, 3599 (1970).

<sup>10</sup>J. H. Barrett, *Phys. Rev.* **86**, 118 (1952).

<sup>11</sup>This limit has been estimated from polarization measurements: L. A. Boatner, U. T. Höchli, and H. Weibel (to be published). The method of crystal growth is also described in this reference.

## Superconductivity of bcc Barium under Pressure

C. Probst<sup>(a)</sup> and J. Wittig

*Institut für Festkörperforschung, Kernforschungsanlage Jülich, D-5170 Jülich, West Germany*

(Received 28 June 1977)

The bcc phase of barium is a superconductor.  $T_c$  increases steeply with pressure from 0.06 K at 37 kbar to 0.5 K at 48 kbar. A fit of McMillan's expression for  $T_c$  suggests a  $T_c$  already in the millikelvin range at 30 kbar. Phonon softening as inferred from the decreasing melting curve is insufficient to account for the rise of  $T_c$  with pressure.

Three high-pressure modifications of barium are known to be superconducting.<sup>1,2</sup> In the phases II and III,  $T_c$  increases from  $\approx 1$  K at 55 kbar to  $\approx 3$  K just before the transformation to the phase Ba IV, which possesses a  $T_c$  of approximately 5.5 K.<sup>2,3</sup> The room-temperature resistivity of Ba II and Ba III increases also considerably under pressure.<sup>1</sup> This is apparently another indication of the steady increase of the electron-phonon interaction with pressure.<sup>4</sup> No superconductivity has been so far observed in the low-pressure bcc phase (Ba I). Interestingly enough, a strong increase of the room-temperature resistivity occurs also in Ba I in the pretransitional range of the transformation to Ba II.<sup>1</sup> The lower straight line in Fig. 1 represents our resistance data for one particular pressure cell. The data are normalized to  $R_{\min}$ , the minimum of  $R(P)$  occurring near 10 kbar. Another interesting property of Ba is the decreasing melting line above 15 kbar and the low melting temperatures in phases II and III.<sup>5,6</sup> Relying on the Lindemann formula, we would like to suggest that the decreasing melting line signals a pressure-induced softening of the average phonon frequencies. Summarizing, the pressure range just below the Ba I-II phase boundary seemed the most probable region in which superconductivity in Ba I could be expected to occur.

We have searched for superconductivity in Ba I under pressure. As indicated by the arrow in Fig. 2, the sample remained normal down to a lowest temperature of 0.05 K at 34 kbar. Between 37 and 48 kbar superconducting transitions were

observed with  $T_c$  varying over an order of magnitude between 0.06 and 0.5 K. The horizontal bars show the pressure distribution as inferred from the width of the superconducting transition of the Pb manometer.<sup>7</sup> The numbers indicate the sequential order of the experiments. It is seen that  $T_c$  depends reversibly on pressure.

In experiment No. 8 (which is missing from Fig. 2) the pressure was increased to 51 kbar at room temperature. The sample transformed partially to Ba II on cooling as seen from a hysteresis loop in the  $R$ - $T$  characteristic. This mixed-phase sample showed a broad superconducting transition between 0.5 and 0.9 K, the latter being

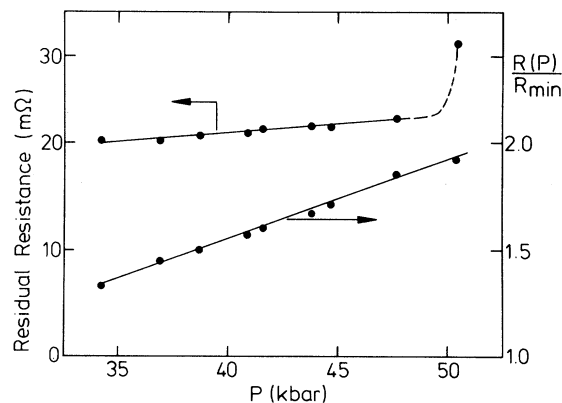


FIG. 1. Room-temperature resistance of bcc Ba vs pressure (lower line). The residual resistance (upper curve) shows a marked increase at the onset of the Ba I  $\rightarrow$  II transition.